LAWRENCE
LIVERMORE
NATIONAL
LABORATORY

UCRL-CONF-221162

Recovery of a CVD diamond detection system from strong pulses of laser produced x-rays

L. S. Dauffy, J. A. Koch, N. Izumi, R. Tommasini, R. A. Lerche

May 7, 2006

High Temperature Plasma Diagnostics
Williamsburg, VA, United States
May 7, 2006 through May 11, 2006

Recovery of a CVD diamond detection system from strong pulses of laser produced x-rays*

L. S. Dauffy, J. A. Koch, N. Izumi, R. Tommasini, R. A. Lerche

Lawrence Livermore National Laboratory, 7000 East Avenue, Livermore, CA 94551

We are studying the response of a CVD diamond detector to a strong x-ray pulse followed by a second weaker pulse arriving 50 to 300 ns later, with a contrast in amplitude of about 1000. These tests, performed at the LLNL Jupiter laser facility, are intended to produce charge carrier densities similar to those expected during a DT implosion at NIF, where a large 14.1 MeV neutron pulse is followed by a weak downscattered neutron signal produced by slower 6-10 MeV neutrons. The number of downscattered neutrons must be carefully measured in order to obtain an accurate value for the areal density, which is proportional to the ratio of downscattered to primary neutrons. The effects of the first strong pulse may include saturation of the diamond wafer, saturation of the oscilloscope, or saturation of the associated power and data acquisition electronics. We are presenting a double pulse experiment that will use a system of several polycrystalline CVD diamond detectors irradiated by 8.6 keV x-rays emitted from a zinc target. We will discuss implication for a NIF areal density measurement.

*This work was performed under the auspices of the U.S. Department of Energy by UC, Lawrence Livermore National Laboratory under Contract No. W-7405-ENG-48.

1. Scope of the experiment

CVD diamond detectors are being investigated for the measurement of the main fuel areal density, ρR, of implosion plasmas during the ignition campaign at the National Ignition Facility, NIF. The areal density is proportional to the ratio of downscattered (6-10 MeV) to primary neutrons (14.1 MeV)[1], thus obtaining a value of ρR requires an accurate measurement of the number of downscattered neutrons (i.e. neutrons scattered inside the deuterium-tritium target). In this work, we are studying the effects of a large pulse recorded by a CVD diamond detector upon a second smaller pulse arriving from 50 to 300 ns later, with a contrast in amplitude of about 1000 (see figure 1). This double pulse experiment will reproduce the case of a DT implosion at NIF, where a large 14.1 MeV neutron pulse is followed by a downscattered neutron signal some tens to hundreds of ns later. Therefore, saturation effects due to this large pulse could have a significant impact on ρR measurements.

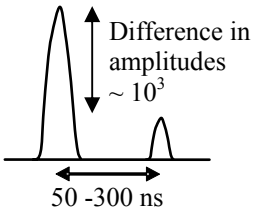

Figure 1. Schematic of the double pulses

The result of such a large pulse on a smaller signal arriving later in time may include saturation of the diamond wafer, of the associated electronics, and of the measuring device (oscilloscope). A previous study has found that the 14 MeV neutrons will not saturate the diamond wafer due to an overproduction of charge carriers (carrier-carrier scattering), even during a successful ignition.[2-4] The saturation of the oscilloscope has also been addressed by building and successfully testing a circuit that clips the first large peak without modifying the signal arriving later in time. The saturation of the associated electronics and other effects are now being quantified during a double pulse experiment. This double pulse experiment is essential in assessing the efficacy of a compact, inexpensive, robust and simple detector for areal density measurement.

2. Ignition charge carrier densities with 8.6 keV x-rays

We are planning to use laser-produced x-rays to generate the double pulses, employing the Comet laser at the LLNL Jupiter Laser Facility. The level of intensity of the two pulses is based on a charge carrier density created

by the x-rays similar to that created by 14.1 MeV neutrons during a DT implosion. It has been determined in a previous work that for a successful ignition, the charge carrier density $D_{e\text{-}h+}$ is equal to 1e15 e^-h^+/cm^3, and for a typical failed ignition, $D_{e\text{-}h+}$ is equal to 3e12 e^-h^+/cm^3. Failed ignition being the main goal of diagnostics, only the failed ignition case will be developed. Using equation 1, we can find that the flux of 8.6 keV x-rays, ϕ_γ, required to produce such a charge carrier density is about 4e8 x-rays/cm^2. The ionization energy in diamond, $\varepsilon_{e\text{-}h+}$, is equal to 13.3 eV/e-h+, and the energy absorption coefficient, μ_{en}, is 12.64 cm^{-1}. The required x-ray fluxes in this work are then about 4e8 x-rays/cm^2 for the large pulse, and about 4e5 x-rays/cm^2 for the smaller pulse.[2]

$$\phi_\gamma = \frac{D_{e-h+}\ \varepsilon_{e-h+}}{E_\gamma\ \mu_{en}} \tag{1}$$

Two laser beams will irradiate a zinc target and produce a flux of 8.6 keV k_α x-rays in 4π space. The angular uniformity of the x-ray flux emitted will be checked by placing several imaging plates at an equivalent distance from the laser/target interaction point, at different angles. Next, the x-ray spectrum incident on the CVD diamond detector's surface will be checked with a CCD camera. This x-ray spectrum, filtered by the beryllium window of the re-entrant tube and by the gold electrodes, will be mostly monoenergetic. Measurement of the output signal, V_{out}, and of the integral under the pulse versus incident energy will then be performed to cross-calibrate the different CVD diamond detectors. The next and main step will be to measure saturation effects using double pulses on three CVD diamond detectors.

3. The Comet laser

We will use a ~6 Joules, 20 ps to 600 ps beam to generate the large pulse, and a ~10 mJ, 500 fs probe beam to generate the smaller pulse. For the long pulse beam, the highest conversion factor (thermal x-rays created per Joule of laser photon, $\xi_{x\text{-}rays}$ = 1e11 x-rays/J) is found at a laser intensity, I, of about 3e16 W/cm^2.[5] For the short pulse beam, the conversion factor (k_α x-rays/J) is comparable over the necessary range of laser intensities (~10^{16} to a few 10^{17} W/cm^2) [6], so we expect to be able to use either short or long pulses interchangeably. We can then obtain the spot radius, r (cm), versus the beam intensity, energy E_{laser} (J), and pulse width τ (s), using equation 2. We want a best focus configuration, i.e about 10 μm diameter laser spot.

$$I = \frac{E_{laser}}{\tau * \pi * r^2} \tag{2}$$

The expected x-ray flux produced at certain distances from the target, L, is equal to $\xi_{x\text{-}rays} * E_{laser} / (4*\pi*L^2)$. Table 1 gives the expected x-ray flux emitted from the zinc target, $\phi_\gamma 1$, and the expected x-ray flux reaching the detection volume, $\phi_\gamma 2$, which is the initial x-ray flux minus about 40% of the flux that is absorbed in the gold electrodes and in the beryllium re-entrant tube window. The charge carrier density and the expected charge created in the detector, in terms of signal's integral, are also given. Note that as explained in reference 1, this signal is not the one observed on the oscilloscope, but rather the one that would be observed if no saturation occurred.[2]

Table 1. Expected x-ray flux at certain distances from the target, L, emitted from the target ($\phi_\gamma 1$) and reaching the detecting volume ($\phi_\gamma 2$), charge carrier density, and the expected signal created in the detector's volume.

L (cm)	$\phi_\gamma 1$ (x-rays/cm^2)	$\phi_\gamma 2$ (x-rays/cm^2)	$D_{e\text{-}h+}$ (e-h+/cm^3)	S (V ns)
4	3.0e9	1.9e9	1.5e13	478 (saturate)
5	1.9e9	1.2e9	9.7e12	306 (saturate)
8	7.5e8	4.7e8	3.8e12	119
10	4.8e8	3.0e8	2.4e12	76

4. The detection system

Three 300 μm thick, 5 mm diameter polycrystalline CVD diamond detectors[7] placed in a 1.3 cm square aluminum casing will be used. A 4 mm diameter hole has been made in the casing to obtain an opening with no

material between the outside and one of the electrodes. A picosecond bias-T is connected to the detector and to the oscilloscope with SMA cables, and to the high voltage with a SHV cable. The high voltage will range from 700 V to about 1000 V. Figure 2 shows the different parts of the detection system.

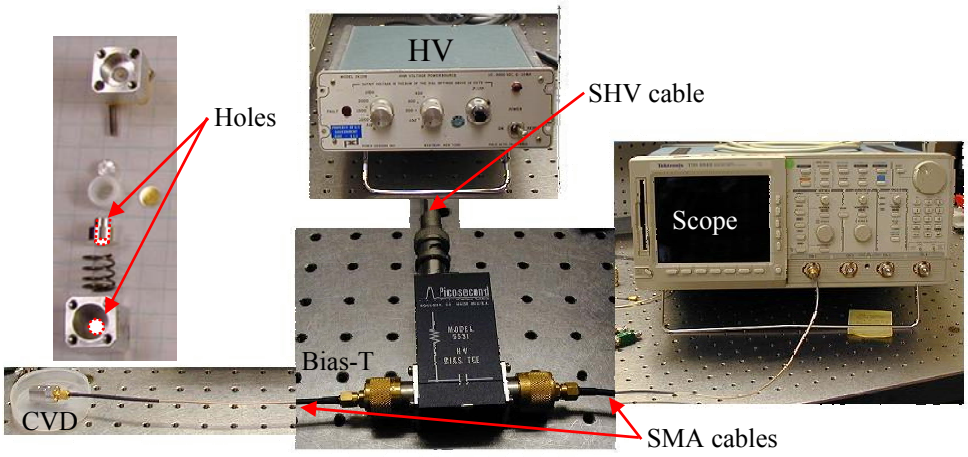

Figure 2. Detection system: CVD diamond detector, bias-T, high voltage supply, oscilloscope.

5. The experiments

The angular uniformity of the x-ray flux emitted will be checked by placing several imaging plates at an equivalent distance from the laser/target interaction point, at different angles. Both the main beam and the probe beam will be tested. Next, the x-ray spectrum will be measured using a CCD camera. An x-ray spectrum produced by a long-pulse laser shot presents discrete K_α lines, whereas that produced by a short-pulse laser shot presents an x-ray spectrum distributed over a large energy range (bremsstrahlung x-rays). X-ray cross sections increase dramatically at low-energies and thus the low-energy part of the spectrum must be removed to avoid energy deposition on only the surface of the detector. The filter used to remove low-energy x-rays will be composed by the electrodes (1 μm gold layer) and by the reentrant tube window (~690 μm of beryllium).

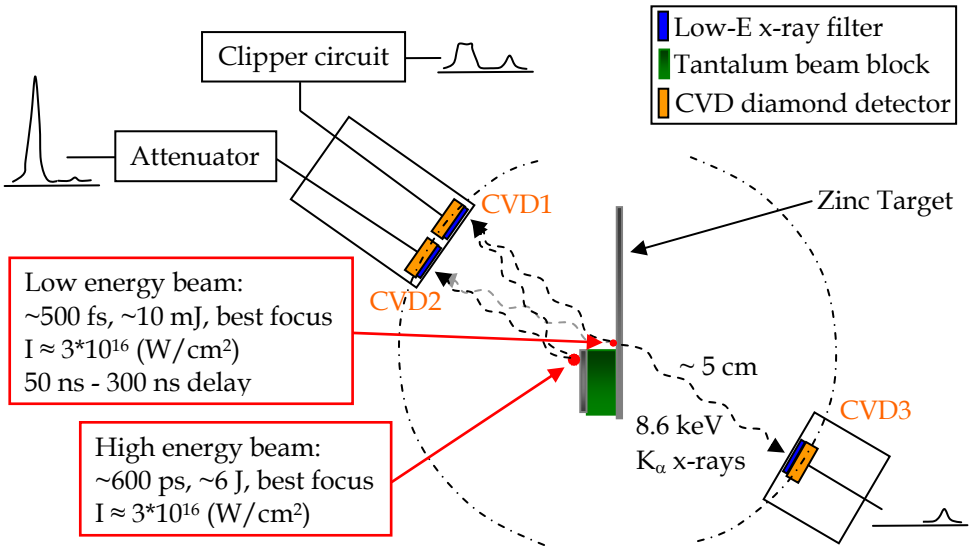

Figure 3. Schematic of the double pulse experiment. Three CVD diamond detectors are inside re-entrant tubes. The zinc target is at chamber center in vacuum.

The output signal (V_{out}, full width half maximum, and the integral under the curve) will then be recorded while increasing the laser energy from a few mJ (probe beam) until about 6 J (main beam). This will allow cross-calibration of the three different CVD diamond detectors so that later comparison of signals recorded by these three detectors during the double pulse test will be possible.

The double pulse experiment set up is described on figure 3. CVD1 and CVD2 will be positioned in air in a re-entrant tube with a ~690 μm window of beryllium. The clipper circuit will be placed between the bias-T and the oscilloscope so that CVD1 will record a clipped first pulse and the second small pulse. CVD2 will be positioned in the same re-entrant tube and an attenuator will be placed before the oscilloscope since the expected large signal will saturate (see table 1). CVD3 will be in a second re-entrant tube and will record only the small pulse since a tantalum beam block will hide the large pulse from CVD3. The high energy beam will shoot first, and the low-energy beam will shoot from 50 ns to 300 ns later. The main interest in this work is to compare the signal recorded by CVD3 (small pulse only) with that recorded by CVD1 (small pulse after clipped large pulse) to quantify the effect of saturation by the large pulse arriving first in time. The delay time between both pulses will be varied from 50 ns to 300 ns to mimic the time delay found between the 14.1 MeV neutrons and the downscattered neutrons (6-10 MeV) during a DT implosion. Different cable lengths and bias-Ts will be used to understand the effects of reflections and bias-T saturation properties.

6. Summary and conclusion

A neutron detection system composed of a CVD diamond, bias-T, high voltage supply, and oscilloscope is being tested to be used at the NIF for areal density measurement. Since areal density is proportional to the ratio of downscattered to primary neutrons, the main challenge in that measurement is the saturation effects caused by a large 14.1 MeV neutron signal on the downscattered neutron signal arriving later in time (50 to 300 ns). To answer that challenge, we are planning to use 8.6 keV x-rays produced by two of the Comet laser beams irradiating a zinc target. A system of 3 CVD diamond detectors and delayed shots will allow seeing the saturation effects of the large first pulse on the smaller pulse. We have addressed oscilloscope saturation using a clipper circuit, and we have explored CVD diamond wafer saturation and we expect it to be negligible. The present work, which is the last step in quantifying the effects of saturation, is crucial to prove that a high- temperature and -flux resistant, simple, compact, and inexpensive detector can measure the areal density during the NIF ignition campaign.

References

1 Wilson D, Mead W, Disdier L, Houry M, Bourgade J, Murphy T: Scattered and (n,2n) neutrons as a measure of areal density in ICF capsules. NUCLEAR INSTRUMENTS & METHODS IN PHYSICS RESEARCH SECTION A-ACCELERATORS SPECTROMETERS DETECTORS AND ASSOCIATED EQUIPMENT **488:** 400-409. 2002.

2 Dauffy L, Koch J: Charge Carrier Density and signal induced in a CVD diamond detector from NIF DT neutrons, x-rays, and electrons. Lawrence Livermore National Laboratory. UCRL-TR-216920. 2005.

3 Nebel C: Electronic properties of CVD diamond. SEMICONDUCTOR SCIENCE AND TECHNOLOGY **18:** S1-S11. 2003.

4 Pan L, Han S, Kania D, Zhao S, Gan K, Kagan H, Kass R, Malchow R, Morrow F, Palmer W, White C, Kim S, Sannes F, Schnetzer S, Stone R, Thomson G, Sugimoto Y, Fry A, Kanda S, Olsen S, Franklin M, Ager J, Pianetta P: Particle-Induced and Photoinduced Conductivity in Type-IIA diamonds. JOURNAL OF APPLIED PHYSICS **74:** 1086-1095. 1993.

5 Matthews D, Campbell E, Ceglio N, Hermes G, Kauffman R, Koppel L, Lee R, Manes K, Rupert V, Slivinsky V, Turner R, Ze F: Characterization of Laser-Produced Plasma X-ray Sources For Use In X-ray Radiography. JOURNAL OF APPLIED PHYSICS **54:** 4260-4268. 1983.

6 Dunn J, Young BK, Hankla A, Conder A, White W, Stewart R: Study of Supra-thermal Electrons and K-α X-rays from High Intensity 500 fs Laser-Produced Plasmas. *In*: 12th International Conference on Laser Interaction and Related Plasma Phenomena. Osaka, Japan. 1995.

7 Tapper R: Diamond detectors in particle physics. REPORTS ON PROGRESS IN PHYSICS **63:** 1273-1316. 2000.